

Temperature-dependent correlation function of magnetoconductance quantum fluctuations in a stadium quantum dot

Dae-Jeong Kim,¹ Jong-Jean Kim,^{1,*} Kyoung Wan Park,² and Hyuk Chan Kwon³

¹*Physics Department, Korea Advanced Institute of Science and Technology, Taejeon 305-701, Korea*

²*Basic Research Department, Electronics and Telecommunications Research Institute, Taejeon 305-600, Korea*

³*Quantum Metrology Division, Korea Research Institute of Standards and Science, Taejeon 305-600, Korea*

(Received 22 August 2001; published 30 January 2002)

The temperature dependence of weak localization and conductance fluctuations in a ballistic quantum dot stadium was studied, where the experimental data of measurements could be best fitted by including both dephasing effects of electron scatterings and thermal smearing of the states around the Fermi energy. We observed a crossover change in correlation function of fluctuations from a Lorentzian-squared form to a simple Lorentzian form as temperature was changed from low-temperature (50 mK) to high-temperature (300 mK) regimes.

DOI: 10.1103/PhysRevB.65.075314

PACS number(s): 73.21.La, 72.15.Gd, 73.20.Fz, 73.50.Td

I. INTRODUCTION

Quantum interference of electrons is exhibited in the low-temperature conductance measurements of mesoscopic electronic devices. Since the phase coherence of conduction electrons is retained over correlation length, it is natural to expect quantum interference to appear in a conductor with dimensions smaller than the phase coherence length. From numerous theoretical and experimental studies conductance fluctuation (CF) and weak localization (WL) have been well understood as the main quantum corrections to conductance of correlated electrons.¹ Those effects in quantum dot cavities generating classical chaos, for example, introduce quantum chaos in the dynamics of ballistic electrons scattered from their boundaries.² Quantum chaos in such cavities has been given an experimental evidence by a characteristic exponential distribution of areas enclosed by electron trajectories and scars of unstable periodic orbits in good agreement with theoretical predictions.²⁻⁵ Random matrix theory (RMT) predicts universal magnitudes of CF and WL effects, where the universality of the magnitudes is derived from statistics of the scattering matrices coupling bound states of the quantum cavities to propagating modes of the conducting leads.^{6,7} Nonetheless, measured magnitudes of the interference effects were far off the theoretical universal values and promoted many works to find a thermal origin of suppression in the magnitudes of the quantum effects at finite temperatures.⁸⁻¹⁰ Within the framework of RMT the deviations of measured values from the universal magnitudes could be explained for the case of WL effect by including a decoherence term since finite temperature cannot affect the WL magnitudes by anything other than diminishing phase coherence length with raising temperature.² However, since thermal broadening and smearing around Fermi energy contribute significantly to transport channels in the mesoscopic devices, reduction of CF magnitude with increasing temperature may also contain those thermal origins of decoherence, smearing, etc. Experimental studies have not been aimed to separate between different finite-temperature effects. In this work we study effects of finite temperature on quantum

transports of electrons in a mesoscopic device and obtain correlation functions of magnetoconductance fluctuations in two limiting temperature regimes to show that thermal smearing of Fermi energy brings about a qualitative change in the correlation. In the low-temperature regime we have obtained a Lorentzian square form for the correlation function: this Lorentzian square form is a characteristic of the CF in the chaotic quantum cavities with exponential distribution of areas swept by electron trajectories.¹¹ In the high-temperature regime we have observed a Lorentzian instead of the Lorentzian square form for the correlation function in agreement with Efetov's theoretical prediction¹² that thermal smearing could affect the correlation function in a qualitative nature. We could obtain by adding a thermal smearing term as well as a dephasing term a better fit to the experimentally obtained correlation functions.

II. EXPERIMENT

The magnetoconductance measurements were carried out using a two-dimensional electron gas located 850 Å below the surface of GaAs/Al_{0.3}Ga_{0.7}As heterojunction wafer with a Si- δ doping of concentration 10^{18} cm⁻³. The wafer was patterned into a Hall bar geometry using wet chemical etching with 150- μ m width and 200- μ m separation of voltage probes. A carrier concentration $n = 3.6 \times 10^{11}$ cm⁻² was measured from the amplitude modulations of the Aharonov-Bohm oscillation at magnetic fields above 1 T at a dilution refrigerator temperature of 50 mK to give mobility $\mu = 3.9 \times 10^5$ cm²/(V s), Fermi wavelength $\lambda_F = 39$ nm, and Fermi energy $E_F = 12$ meV. The stadium quantum cavity was prepared by using Ti/Au (40 Å/200 Å) electrostatic gates defined on the Hall bar structure. The stadium dot, shown in Fig. 1, has dimensions 0.65×1.25 μ m², after accounting for ~ 70 nm depletion edge, giving ~ 0.68 μ m² effective area. The point contacts of split gates all have a lithographic width ~ 200 nm and allow conductance to be tunable independently with a desirable number of transverse modes of the conductance quantization. The distance between split gates was kept to be below ~ 100 nm to prevent leakage of electrons around the stadium edge. The direct-through trajectory

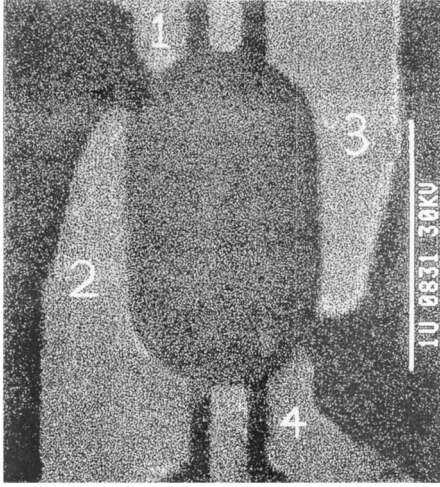


FIG. 1. Scanning electron microscopic image of our quantum dot stadium with split gate structures.

ries, which would bias the statistics of fluctuations, were avoided by off-line displacement between the entrance and exit point contacts. Magnetoconductance measurements were carried out at a dilution refrigerator temperature down to 50 mK using standard ac lock-in techniques. The magnetic field oriented perpendicular to the plane of electron gas was swept to a precision of ± 0.02 mT. A four-probe configuration with a current source of 0.2 nA at 27 Hz was employed to avoid excessive heating of conducting electrons.

III. RESULTS AND DISCUSSION

Figure 2 shows two magnetoconductance plots of the stadium cavity measured for three allowed modes in the point contacts at dilution temperatures of $T=300$ mK and 5.4 K,

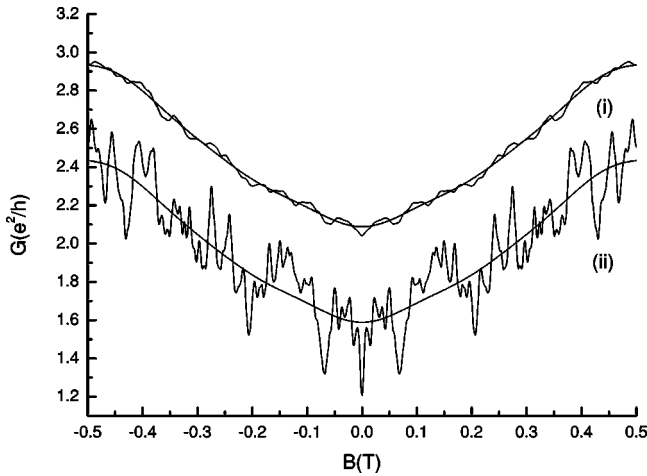


FIG. 2. Magnetoconductance of a stadium quantum cavity with three transmission modes ($N=3$) at both entrance and exit quantum point contacts. Trace (i) has an offset $0.5e^2/h$ for a convenient comparison and represents the data at 5.4 K. Trace (ii) was obtained at 300 mK with the same bias voltage as in (i). These aperiodic fluctuations are highly reproducible over consecutive measurements and highly symmetric $G(+B) \approx G(-B)$. Solid lines in both traces are mean value backgrounds.

respectively. The magnetoconductance plots are symmetric with respect to the magnetic field reversal as expected from the Onsager's relation for two-probe measurements with the Hall bar geometry.¹ The Hall bar has macroscopic dimensions and the probes are not phase invasive so that the measured conductance fluctuations may be all attributed to the stadium cavity effect. Data at low temperature ($T=300$ mK) exhibit notable aperiodic fluctuations due to quantum interference between forward-scattered electrons. Such an interference effect on the conductance is greatly suppressed at high temperature ($T=5.4$ K). The smoothing out of fluctuations at higher temperature is due to the reduction of the phase coherent length of conducting electrons and also uncorrelated electrons thermally activated around the Fermi energy. In Fig. 3 we show conductance dips observed at zero magnetic field in the stadium cavity for two and three allowed modes of the point contacts. Applying a small magnetic field can easily destroy the time reversal symmetry (TRS) of the electron path and wash out the conductance dips of the WL effect. RMT predicts the shape function of the WL dip^{3,7,13} as

$$\langle \Delta G(B) \rangle = \frac{-\Delta g}{1 + (B/B_c)^2} \quad \text{with} \quad \Delta g = \frac{N}{2N + N_\phi} \frac{e^2}{h}, \quad (1)$$

where B_c defines the localization field scale that characterizes a distribution of the areas enclosed by pairs of time reversal paths and thus depends on size and shape of the cavities. RMT determines the WL strength Δg in terms of the number of allowed modes at contacts N ($N \gg 1$) and effective phase breaking channels N_ϕ .¹³ From the above expression of Δg the WL correction can be seen to reduce to $0.5e^2/h$ for a perfect phase coherence at zero temperature. We can fit our measurements to this functional form with two parameters of Δg and B_c as shown in Fig. 3. For the case of two modes ($N=2$) at $T=50$ mK [Fig. 3(a)], the WL strength Δg and field scale B_c are obtained as $0.35e^2/h$ and 2.8 mT, respectively. The WL strength $0.30e^2/h$ and field scale 2.6 mT are obtained for the same two-mode ($N=2$) case but at $T=300$ mK [Fig. 3(b)]. At the same temperature of 300 mK we have obtained the WL strength $0.34e^2/h$ and field scale 3.1 mT for the three-mode ($N=3$) case [Fig. 3(c)]. Since the WL is not reduced by thermal smearing but by electron dephasing, the WL effects can be used to calculate the dephasing rate.¹⁴ The numbers of dephasing channels at $T=300$ mK are obtained as $N_\phi=2.6$ for $N=2$ and 2.8 for $N=3$, respectively. At a lower temperature $T=50$ mK, $N_\phi=1.7$ is obtained for $N=2$. The phase coherent lengths are estimated from the Hall bar measurements as 7 μm at 300 mK and 12 μm at 50 mK. The reduction of the phase coherent length with increasing temperature was already reported in previous experimental works.^{6,7} Although the theoretical values predicted by RMT should be compared more reasonably with averages over statistical ensembles generated by shape distortions or electron energy changes, our results of N_ϕ are compatible with the results of conductance measurements at different mode numbers (N) but the same temperature. Following a semiclassical analysis the field

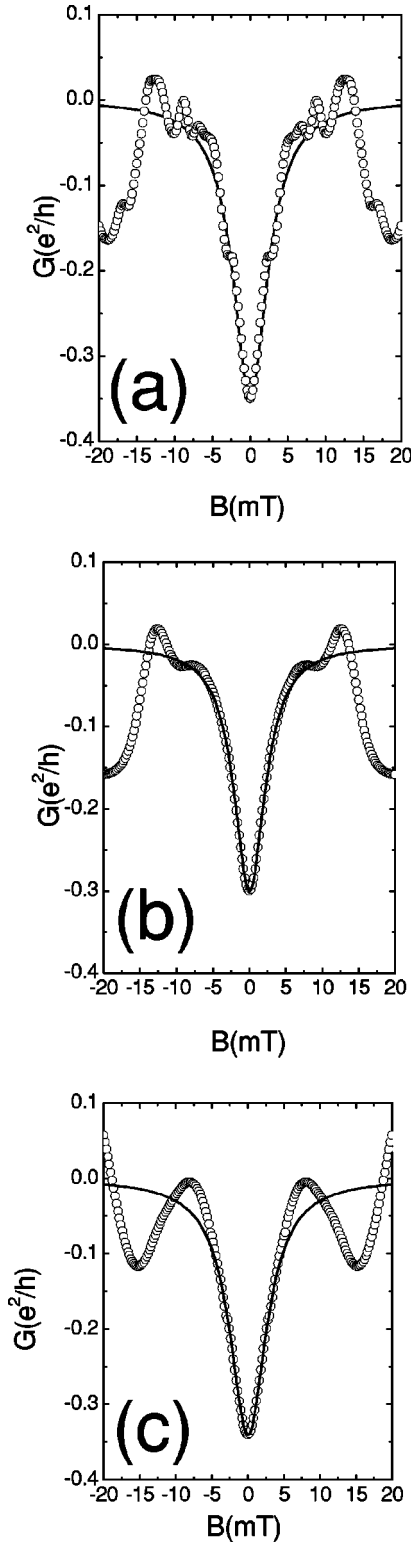


FIG. 3. Conductance dips corresponding to the weak localization in the stadium: (a) observed for $N=2$ at $T=50$ mK, the solid line is a best fit by an inverted Lorentzian square with $\Delta g = 0.35e^2/h$, $B_c = 2.8$ mT, (b) observed for $N=2$ at $T=300$ mK, the solid line is a best fit by an inverted simple Lorentzian with $\Delta g = 0.30e^2/h$, $B_c = 2.6$ mT, and (c) observed for $N=3$ at $T=300$ mK, the solid line is a best fit by an inverted simple Lorentzian with $\Delta g = 0.34e^2/h$, $B_c = 3.1$ mT.

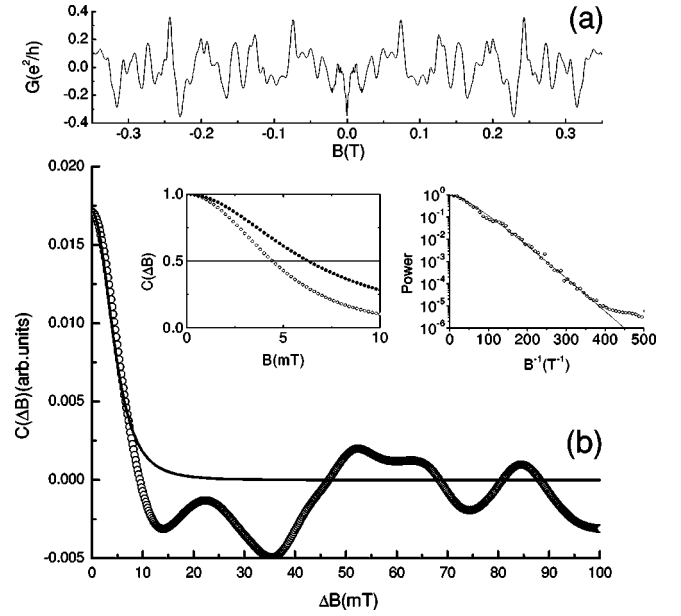


FIG. 4. (a) Conductance fluctuations in the stadium quantum cavity measured with two transmission modes ($N=2$) at $T=50$ mK and (b) correlation function of fluctuations best fitted by a Lorentzian square form (solid line). The correlation function was calculated from the data (a) in the range of B from 0.02 mT to 0.35 T. The left inset shows two correlation functions at $T=50$ mK ($\circ\circ\circ$) and $T=300$ mK ($\bullet\bullet\bullet$) respectively. The right inset shows a Fourier transform power spectrum of fluctuations at $T=50$ mK, where the solid line represents a fit by an exponential.

scale $B_c \sim 3$ mT seems appropriate when we consider that our device has an effective area of $0.68 \mu\text{m}^2$ with depletion edge and requires a magnetic field strength ~ 6 mT to increase by one flux quantum through the effective area. The field scale B_c roughly corresponds to the magnetic field required to increase the flux through the area of the cavity by one-half flux quantum. It may be that the electrons, which contribute to the WL effect, traverse along the trajectories, threading similar areas of the cavity, to return to their initial positions and a pair of time reversal symmetric paths encloses effectively twice the area. B_c thus corresponds to a field strength to add one quantum flux through the area that a pair of time reversal symmetric electron trajectories are threading around. We can obtain fluctuations originated purely from quantum interference by subtracting out a smooth fit of the high-temperature ($T=5.4$ K) data as a background where quantum interference effects are mostly suppressed. Figures 4(a) and 5(a) show the pure conductance fluctuation data for the stadium cavity at 50 mK and 300 mK with two and three allowed modes (in units e^2/h), respectively, at the point contacts, corresponding to a relatively low magnetic field so that the cyclotron radius becomes too large to bring about edge-state formation.

To analyze statistical properties of these CF data, we examine the correlation function of magnetoconductance fluctuations defined as below and depicted in Figs. 4 and 5(b):

$$C(\Delta B) = \langle \delta G(B + \Delta B) \delta G(B) \rangle \quad (2)$$

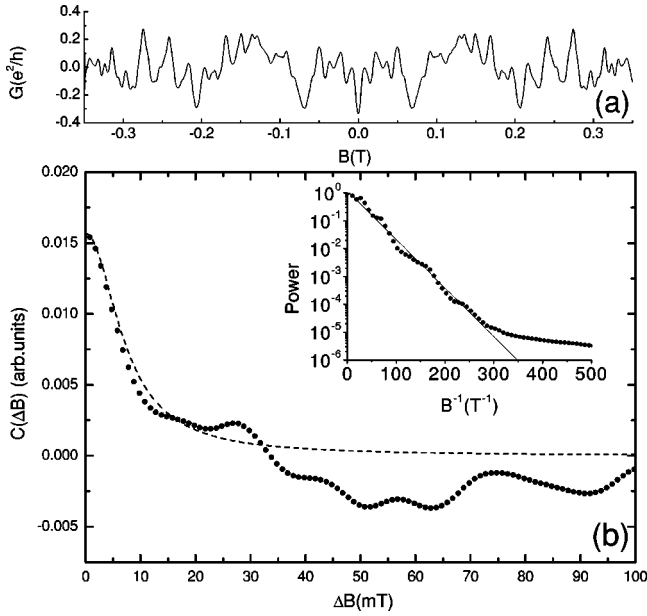


FIG. 5. (a) Conductance fluctuations in the stadium quantum cavity measured with three transmission modes ($N=3$) at $T=300$ mK and (b) correlation function of the fluctuations best fitted by a simple Lorentzian form (dashed line). The inset shows a Fourier transform power spectrum.

where δG represents $G(B) - \langle G(B) \rangle$ in units of e^2/h , B the magnetic field, and the brackets an average over a suitable range of field from 0.02 mT to 0.34 mT. Using the supersymmetry algebra Efetov⁹ derived, with considerations of both thermal smearing and dephasing, the asymptotic forms of the correlation function in the limiting temperature regimes. In the low-temperature regime the theory is consistent with the RMT result in the prediction of magnitude of CF but with the semiclassical approach³ in the prediction of its Lorentzian square form of the correlation function, conforming to the exponential distribution of areas threaded by electron trajectories,

$$C(\Delta B) = \frac{C(0)}{[1 + N_\phi/2N + (\Delta B/B_\alpha)^2]^2},$$

$$P(\omega) = P(0) [1 + 2\pi\sqrt{1 + N_\phi/2NB_\alpha}\omega \times \exp[-2\pi\sqrt{1 + N_\phi/2NB_\alpha}\omega], \quad (3)$$

where $B_\alpha = \alpha\phi_0$ represents the correlation field scale, $P(\omega)$ power spectrum of fluctuations, ω frequency, and $C(0)$ assumes $1/16$ at zero-temperature limit.⁷ The inset of Fig. 4(b) shows a normalized power spectrum for the two-mode ($N=2$) case at 50 mK, where the low-temperature criterion $2\pi^2k_B T \ll N\varepsilon$ (ε is the mean level spacing) is satisfied. The parameter B_α corresponds to the magnetic field strength for adding one quantum flux through the area that electrons injected from the entering point contact thread during passage to the exit point contact. We have obtained $B_\alpha \approx 5.5$ mT for the $N=2$ case from best fitting the data to the correlation function $C(\Delta B)$ and power spectrum $P(\omega)$ of Eq. (3). This B_α value is almost twice the value $B_c \approx 2.8$ mT of the WL

effect for the same $N=2$ and same temperature. This interesting relationship of $B_\alpha \approx 2B_c$ can be understood from the fact that the average area enclosed by electron trajectories of the WL effect is twice that of conductance fluctuations within the semiclassical picture.¹⁵ The Lorentzian square curve of correlation functions and the exponential form of power spectrum of the magnetoconductance fluctuation were already observed in other experimental works.^{14,16} A Lorentzian square correlation function with a universal magnitude of CF in chaotic quantum cavities with exponential distribution of threading area A , $P(A) \propto \exp(2\pi\alpha A)$, was derived under the assumption that the electrons were perfectly coherent and their temperature was so low that thermal smearing should not have any significant contribution to the conductance properties. The left inset of Fig. 4(b) shows the evolution of the correlation function with increasing temperature. Compared with the correlation function at low temperature ($T=50$ mK), the correlation function at high temperature ($T=300$ mK) has a broader width, and a best fit by Eq. (3) gives $B_\alpha \approx 6.9$ mT larger than the value 5.2 mT expected from $B_c \approx 2.6$ mT obtained from the WL measurement at 300 mK. For $N=3$ and $T=300$ mK, where the high-temperature condition $2\pi^2k_B T \gg N\varepsilon$ holds, we could fit the experimental data by Eq. (3) to obtain $B_\alpha \approx 8.4$ mT. Referring to the value of $B_c \approx 3.1$ mT obtained from the WL, it is also larger than expected from the $B_\alpha \approx 2B_c$ relation. These larger B_α values cannot be understood from a simple semiclassical picture.^{3,15} However, following Efetov,¹² this larger B_α may not originate from a scattering redistribution of electron trajectories but by a thermal smearing that affects more for the longer electron trajectories of chaotic cavities. From the supersymmetry-based theory the correlation function of magnetoconductance and its power spectrum in the high-temperature regime are known to take the following forms,¹² respectively:

$$C(\Delta B) = \frac{N\varepsilon}{24k_B T} \frac{1}{1 + N_\phi/2N + (\Delta B/B_\alpha)^2},$$

$$P(\omega) = P(0) \exp[-2\pi\sqrt{1 + N_\phi/2NB_\alpha}\omega]. \quad (4)$$

The above equations take into account not only a smearing of the Fermi distribution but also a dephasing of electrons by inelastic scattering. In Fig. 5(b) we show the correlation function of magnetoconductance fluctuations and its power spectrum for $N=3$ and $T=300$ mK. The best fit to a simple Lorentzian, Eq. (4), instead of the Lorentzian square, Eq. (3), with $B_\alpha \approx 6.0$ mT was more satisfactory. At $T=300$ mK the simple Lorentzian fit was good also for $N=2$ with $B_\alpha \approx 5.1$ mT. Meanwhile, in the earlier experiments the correlation field scale B_α obtained by fitting to Eq. (3) was shown to be temperature independent.¹⁶ This surprising change of correlation function from a Lorentzian square to a simple Lorentzian with the same B_α manifests importance of broadening in available states near Fermi energy in the high-temperature regime, which increases inelastic collisions of additional phase shifts. This thermal broadening thus leads to additional dephasing of electrons and thus loss of phase information. The variances of CF are obtained as 0.010 for N

$=2$ and 0.015 for $N=3$. When we compare these results with the theoretical prediction $N^2\varepsilon/12k_B T(2N+N_\phi)$ of Eq. (4), which includes the dephasing rate N_ϕ derived from the WL measurement, we can obtain the electron temperature of 320 mK for both $N=2$ and $N=3$ in conformity with the sample temperature. These results suggest two major effects of thermal origin at high temperatures, where inelastic scattering of thermal origin can be a dominant source to suppress the CF.

IV. CONCLUSION

Our measurements on magnetoconductance of a quantum dot stadium at finite temperature show that thermal smearing

effects are very important to understand the experimental conductance data. We found that the correlation function evolved from a Lorentzian square at low temperature to a simple Lorentzian at high temperature with constant B_α in good agreement with theoretical predictions of Efetov.¹² The best fit to the experimental data could be made better by a formula which includes both the dephasing effect and thermal smearing as a dominant source to suppress the quantum interference effects.

ACKNOWLEDGMENTS

This work was supported in part by the KAIST Chair Fund from the Korea Telecom endowment.

*Corresponding author. Electronic address: jjkim@cais.kaist.ac.kr

¹D.K. Ferry and S.M. Goodnick, *Transport in Nanostructures* (Cambridge University Press, Cambridge, England, 1997); S. Datta, *Electronic Transport in Mesoscopic System* (Cambridge University Press, Cambridge, England, 1995).

²C.M. Marcus, S.R. Patel, A.G. Huibers, S.M. Cronenwett, M. Switkes, I.H. Chan, R.M. Clarke, J.A. Folk, S.F. Godijn, K. Campman, and A.C. Gossard, *Chaos, Solitons Fractals* **8**, 1261 (1997).

³H.U. Brauger, R.A. Jalabert, and A.D. Stone, *Phys. Rev. Lett.* **70**, 3876 (1993).

⁴M.C. Gutzwiller, *Chaos in Classical and Quantum Mechanics* (Springer, New York, 1990).

⁵J.P. Bird *et al.*, *Phys. Rev. Lett.* **82**, 4691 (1995).

⁶C.W.J. Beenakker, *Rev. Mod. Phys.* **69**, 741 (1997).

⁷H.U. Baranger and P.A. Mello, *Phys. Rev. Lett.* **73**, 142 (1994).

⁸A.G. Huibers, J.A. Folk, S.R. Patel, C.M. Marcus, C.I. Duruoz, and J.S. Harris, *Phys. Rev. Lett.* **83**, 5090 (1999).

⁹A.G. Huibers, M. Switkes, C.M. Marcus, K. Campman, and A.C. Gossard, *Phys. Rev. Lett.* **81**, 200 (1998).

¹⁰D.-J. Kim, J.-J. Kim, K.W. Park and H.C. Kwon, *Phys. Rev. B* **64**, 81305 (2001).

¹¹H.U. Baranger, R.A. Jalabert, and A.D. Stone, *Chaos* **3**, 665 (1993).

¹²K.B. Efetov, *Phys. Rev. Lett.* **74**, 2299 (1995).

¹³H.U. Baranger and P.A. Mello, *Phys. Rev. B* **51**, 4703 (1995).

¹⁴C.M. Marcus, R.M. Westervelt, P.F. Hopkins, and A.C. Gossard, *Phys. Rev. B* **48**, 2460 (1993).

¹⁵M.J. Berry, J.H. Baskey, R.M. Westervelt, and A.C. Gossard, *Phys. Rev. B* **50**, 8857 (1994).

¹⁶J.P. Bird, K. Ishibashi, D.K. Ferry, Y. Ochiai, Y. Aoyagi, and T. Sugano, *Phys. Rev. B* **52**, 8295 (1995).